Meteoritics & Planetary Science 40, Nr 7, 1023–1042 (2005)
Abstract available online at http://meteoritics.org

A Mössbauer spectroscopy and X-ray diffraction study of ordinary chondrites: Quantification of modal mineralogy and implications for redox conditions during metamorphism

O. N. MENZIES[1, 2], P. A. BLAND[1, 3*], F. J. BERRY[2], and G. CRESSEY[3]

[1]Impacts & Astromaterials Research Centre (IARC), Department of Earth Science and Engineering, South Kensington Campus, Imperial College, London SW7 2AZ, UK
[2]Department of Chemistry, The Open University, Walton Hall, Milton Keynes MK7 6AA, UK
[3]Department of Mineralogy, The Natural History Museum, Cromwell Road, London SW7 5BD, UK
[*]Corresponding author. E-mail: p.a.bland@imperial.ac.uk

(Received 30 May 2003; revision accepted 21 October 2004)

Abstract–We present a method that combines Mössbauer spectroscopy and X-ray diffraction to quantify the modal mineralogy of unequilibrated ordinary chondrites (UOCs). Despite being a fundamental tool in the interpretation of geological systems, there are no modal mineralogical data available for these meteorites. This is due to their fine-grained nature, highly heterogeneous silicate mineralogy, and the presence of poorly characterized phases. Consequently, it has not been possible to obtain accurate modal mineralogy by conventional techniques such as point counting.

Here we use Mössbauer spectroscopy as a preliminary identification technique and X-ray diffraction provides the quantification for a suite of recent UOC falls. We find the most primitive UOCs to contain a significant amount of phyllosilicate material that was converted during metamorphism to form ferromagnesian silicates. A complete suite of Antarctic samples is analyzed by each method to observe mineralogical trends and these are compared with trends shown by recent falls. The fact that mineralogical relationships shown by finds and falls are in agreement allows us to be confident that we are observing the products of pre-terrestrial alteration.

Mössbauer spectroscopy reveals evidence of steadily increasing reduction with metamorphism in the UOCs. Because this technique allows comparisons to be made between UOCs and EOCs, our reduction sequence can be combined with other evidence showing progressive oxidation in the EOCs. This yields an integrated model of changing redox conditions on equilibrating ordinary chondrite parent bodies.

INTRODUCTION

The unequilibrated ordinary chondrites (UOCs), along with the carbonaceous chondrites, are some of the most primitive materials in the solar system (e.g., Dodd et al. 1967). Much work has been carried out on their chemistry and isotopic compositions (e.g., Jarosewich 1966, 1990; Dodd et al. 1967; van Schmus and Wood 1967; Dodd 1981; Sears and Weeks 1986; Clayton et al. 1991). These data have provided a means of classifying ordinary chondrites as well as investigating conditions on meteorite parent bodies. Several aspects of ordinary chondrite parent body processes have aroused substantial controversy in recent times. These include the growing evidence of aqueous alteration in UOCs and conditions of metamorphism, particularly with regard to reduction and oxidation.

DuFresne and Anders (1961) first suggested that aqueous alteration was a significant process on carbonaceous chondrite parent bodies. Hutchison et al. (1987) were first to describe the presence of pre-terrestrial smectite in an ordinary chondrite, indicating that the parent material of both ordinary and carbonaceous chondrites underwent hydrothermal alteration. Zolensky and McSween (1988) gave a thorough review of the processes and products of aqueous alteration of chondrites. Evidence for widespread aqueous alteration on ordinary chondrite parent bodies was provided by Grossman et al. (2000) in their study of "bleached chondrules." They proposed that these textures were formed by low temperature aqueous alteration in all ordinary chondrites before any thermal metamorphism occurred. Bland et al. (2002) have developed an alteration index based on the quantification of carbonaceous chondrite alteration products. However the

location of alteration, whether nebular or parent body, is still an unresolved issue (e.g., Sears and Akridge 1998).

Larimer (1968) was among the foremost to suggest that some reduction may have occurred during ordinary chondrite metamorphism. He based his observations on the fact that the most primitive meteorites, believed to have formed under oxidizing conditions, also contained metallic Fe. He proposed that the redox states of ordinary chondrites were set in the solar nebula. Heyse (1978) argued that lower petrologic types (i.e., meteorites of low metamorphic grade, van Schmus and Wood 1967) are the more reduced chondrites. However, Brett and Sato (1984) measured intrinsic oxygen fugacities of five ordinary chondrites and found that equilibrated ordinary chondrites (EOCs) were more reduced than the UOCs. They proposed a parent body setting for reduction with graphite as the reducing agent and that this reaction would have ceased as elemental carbon dissolved in metal at high temperatures. McSween and Labotka (1993) gave a summary of the contrasting hypotheses that have existed regarding redox conditions on ordinary chondrite parent bodies since 1968. Their conclusion was that although the UOCs contain some evidence of reduction, progressive oxidation with metamorphism was the dominant process that affected the EOCs. They asserted that the confusion over what redox conditions prevailed arose from making comparisons between UOCs and EOCs. More recently Gastineau-Lyons et al. (2002) have used silicate ratios to confirm that oxidation increases with metamorphism in L and LL EOCs.

There are a number of means by which redox conditions could be assessed. One important parameter that has been somewhat overlooked is the abundance of specific mineral phases. The fine-grained nature of primitive unequilibrated chondrites, combined with their complex heterogeneic mineralogy, makes phase quantification difficult to achieve by conventional means, i.e., using an electron microprobe or by simple point counting (e.g., Dodd et al. 1967). To date no quantitative modal analysis of UOCs has been published. Dorfler and Hiesbock (1969) investigated a means of assessing the quantitative mineralogy of ordinary chondrites using stereometric analysis. However, this work encountered grain-size obstacles and was never pursued. Such mineralogical information would be invaluable in building up a geological history of primitive meteorites and ultimately in interpreting early solar system processes.

Dodd (1969) gave an overview of the variation in mineralogy of the ordinary chondrites with petrologic type. The study looked at the changes in chemical composition of minerals with metamorphism, rather than the variation in mineral abundance and did not include the subtle changes that occurred during equilibration within the UOCs, as a metamorphic scale for these meteorites did not exist at the time. There is a need for both approaches, changes in mineral composition and abundance, to be combined in order to create a valid model of changing conditions on equilibrating ordinary chondrite parent bodies. Dodd (1981) asserted that there is a close correspondence between the normative and modal mineralogy of ordinary chondrites, as defined by electron microprobe analysis, with “minor exceptions” in the UOCs.

McSween et al. (1991) made normative calculations of 94 ordinary chondrites in an attempt to correlate meteorite mineralogy with asteroid composition from reflectance spectra. Gastineau-Lyons et al. (2002) consolidated this work for the EOCs and asserted that normative mineralogy is not a direct analogy for modal mineralogy of ordinary chondrites.

With the growing interest in aqueous alteration on meteorite parent bodies and observations of phyllosilicates and other hydrous alteration products in ordinary chondrites, we believe that the use of a normative anhydrous mineral suite to represent UOC mineralogy is insufficient and have explored other means of constraining UOC mineralogy. Bland et al. (2004) have recently presented a unique instrumental solution to this problem using a combination of Mössbauer spectroscopy and X-ray diffraction to quantify carbonaceous chondrite mineralogy. Here we take a similar approach.

Iron-57 Mössbauer spectroscopy has been used to investigate the mineralogy of chondritic meteorites by detecting Fe bound in a crystal lattice (Sprenkel-Segel and Hanna 1964). The technique investigates the oxidation state and electronic configuration of Fe atoms in minerals. Sprenkel-Segel and Hanna (1964) were among the first to use this method to investigate meteorites; they analyzed several chondrites using Mössbauer spectroscopy and compared the absorption patterns obtained with those for reference terrestrial minerals in order to identify the meteoritic components. They found that it was possible to identify the Fe-bearing minerals present, the oxidation state of the Fe, and the relative proportions of the minerals. Also, the mineral compositions could be better estimated than by normative calculations from chemical analyses.

The various mineral components observed in spectra of rocks or meteorites are identified by their unique Mössbauer parameters. Mössbauer spectroscopy can also be used quantitatively to yield wt% values of Fe-containing minerals, where the Fe content of the mineral is known (Meisel et al. 1990; Fegley et al. 1995; Bland et al. 1998), i.e., it is easier to quantify the wt% of magnetite which has a uniform composition than olivine which in primitive chondrites is highly heterogeneous. It is a particularly useful tool because the individual mineral components are analyzed in a non-destructive manner (Herr and Skerra 1969), which is important when analyzing small and precious pieces of meteorite. Mössbauer spectroscopy is capable of detecting even poorly crystalline phases with grain sizes larger than approximately 10 nm and Bland and Cressey (2001) have shown that it can detect the presence of Fe-bearing minerals of abundance >1 wt%. Although it is possible to convert Mössbauer “percentage of fit” values to wt% units for

minerals of known Fe content, such as troilite and magnetite, this is not always an option for minerals with such heterogeneous compositions as those found in chondrites. Consequently, Mössbauer spectroscopy is used here primarily as an identification technique for fine-grained, Fe-containing phases.

In addition, specific Mössbauer parameters, reflecting the chemical environment of electrons at the nucleus, can be used to provide information on sample composition. Menzies et al. (2001) have used this technique to investigate the olivine solid solution series and thus to make observations about the EOCs which have fixed and known olivine compositions. In this study we go on to further explore this relationship and its application to the more complex UOCs.

X-ray diffraction (XRD) has long been used to identify crystalline phases in rocks and meteorites (DuFresne and Anders 1961). Traditionally, quantitative analysis has been carried out using reference intensity ratio (RIR) methods which utilize either internal or external standards (e.g., Chung 1974a, b). More recently, whole pattern fitting techniques (e.g., Rietveld methods) that require substantial data processing have been implemented (e.g., Hill and Howard 1987; Smith et al. 1987; Bish and Howard 1988).

Our experimental procedure utilizes a 120° curved position-sensitive detector (PSD), the deliberate use of a copper source, and a novel sample preparation method developed by Cressy and Schofield (1996). The technique allows quantitative analysis to be carried out even on mixtures containing phases that cause preferred-orientation effects such as clays (Batchelder and Cressey 1998), which is of significant benefit in the analysis of primitive meteorites. The quantification method utilizes the entire powder pattern and its Fe content, thus minimizing the effect of enhanced intensity peaks caused by preferred orientation (Cressey and Schofield 1996). Cressey and Schofield (1996) carried out "blind" tests on mechanical mixtures of known, weighed amounts of different minerals. The total time taken for the quantitative assessment of three-phase mixtures was 15 min and the average difference between the actual and measured wt% was 1.4%, showing that this technique allows fast and efficient, quantitative assessment of multiphase samples. Schofield et al. (2002) have compared the technique to the more labor-intensive Rietveld method using neutron powder diffraction for mantle harzburgites, and the results obtained were identical within error. Bland et al. (2004) have refined this method; using it to quantify the modal mineralogy of carbonaceous chondrites. They provide full details of the experimental methodology and unique problems encountered when applying the technique to unequilibrated samples.

By combining Mössbauer spectroscopy as an identification tool and X-ray diffraction to provide the final quantification, all crystalline Fe-bearing phases can be identified. Non-crystalline Fe-free phases will not be detected using this method, however, they comprise a minor proportion of total ordinary chondrite mineralogy, so this is not considered a serious drawback.

This work presents the integrated use of Mössbauer spectroscopy and X-ray diffraction to quantify the modal mineralogy of both equilibrated and unequilibrated ordinary chondrites. We aim to investigate the trends of changing mineralogy with metamorphism, in order to yield valuable information about early conditions on ordinary chondrite parent bodies.

EXPERIMENTAL METHODS

^{57}Fe Mössbauer Spectroscopy

Mössbauer spectroscopy operates on the principle of resonant absorption of γ rays by Fe nuclei in a sample. The use of a ^{57}Co source allows the presence of ^{57}Fe in meteorite samples to be analyzed. The energy of the source γ rays is Doppler shifted by relative motion between the source and the target absorber. This yields a range of γ ray energies allowing velocity (mm/s) to be plotted against absorption (%).

The energy of a nucleus is influenced by the chemical environment of an atom and can be defined by three Mössbauer parameters. Hence, minerals containing Fe in different forms can be identified by their unique Mössbauer parameters (e.g., Berry 1983). Isomer shift is a parameter measuring s electron density around the nucleus. It can be used to tell the co-ordination numbers of atoms and their oxidation states. Magnetic splitting measures the orientation and magnitude of the magnetic field that may be set up around the nucleus. Quadrupole splitting yields information about the electronic environment of a nucleus and the distribution of atoms in a particle and is the parameter concentrated on in this study. Electron charge is not always spherically distributed around a nucleus. It may have an electric field gradient creating an elliptical distribution. This causes splitting from a one-line to a two-line spectrum. The magnitude of the quadrupole splitting parameter is the distance between the two resulting peaks. Quadrupole splitting occurs in non-cubic minerals and gives information about the environment of the site in which the atom lies. For example, the Fe^{3+} nucleus has a spherical, symmetrical configuration and therefore a small value of quadrupole splitting, while Fe^{2+} is asymmetric owing to the presence of a 6th d electron and a large quadrupole splitting value is observed (Burns 1993).

Analysis of Meteorites

In this study approximately 100 mg of powdered bulk meteorite sample was placed in a lead sample holder and then irradiated for between 24 and 72 hrs at 298 K. The drive velocity was calibrated using a metallic Fe foil. Spectra were fitted with a constrained non-linear least squares fitting program of Lorentzian functions. Integration of the fitted lines gives the relative area intensities of the Fe-containing

phases. The Mössbauer spectra of bulk meteorites are complex, consisting of multiple components. In ordinary chondrites, ^{57}Fe is found in silicate minerals (olivine, low-Ca pyroxene and phyllosilicates), in sulfides (troilite), oxides (magnetite), and as Fe-Ni metal.

X-ray Diffraction

X-ray diffraction provides a rapid means of characterizing and quantifying mineral phases in meteorites in a non-destructive manner and the method utilized here has been described in detail by Bland et al. (2004). The use of a stable, curved, position sensitive detector (PSD) in a fixed geometry allows accurate and reproducible phase quantification of primitive, clay-containing meteorites. In addition to Bragg scattering from the crystalline phases, the $CuK\alpha_1$ (germanium III monochromated) radiation interacts with Fe in the sample causing Fe fluorescence radiation to be emitted. This fluorescence is also detected by the PSD and the resultant pattern is a superimposition of Bragg diffraction peaks on an overall fluorescence background signal. The Fe fluorescence recorded by the PSD has a characteristic undulating signature related to the signal processing electronics, but is a stable and reproducible function. This characteristic fluorescence signal is useful for identifying the amount of Fe in a sample and also for the fitting process (Cressey and Batchelder 1998) described below. Furthermore, it means that this XRD technique allows direct comparison with Mössbauer analysis (Bland and Cressey 2001).

Analysis of Meteorites

The sample was prepared by gently crushing to a fine, smooth powder and placing in a circular plastic well (15 mm diameter, 1 mm deep). With highly fluorescing material it is important to achieve a smooth top surface to the sample, as surface roughness differences between samples and standards can lead to microabsorption that will affect the quantification (Cressey and Batchelder 1998). However, excessive flattening of the surface can impose a preferred orientation effect on tabulate minerals and cause certain Bragg peaks to be enhanced. Details of the sample preparation procedure are outlined in Batchelder and Cressey (1998) and Cressey and Batchelder (1998). Once the sample was properly prepared it was left to acquire counts for 600 min. It has been shown that accurate phase quantification can be carried out on patterns acquired for only 5 min (Cressey and Batchelder 1998), but for the complex, multiphase meteorite samples analyzed here, longer count times ensured that the peak intensities were increased and the background/noise ratio reduced, simplifying the fitting procedure. Silicon was used as an external calibration standard as described by Cressey and Schofield (1996).

The amount of an individual phase present in each sample pattern was estimated by using a computer least-squares fitting program to compare the peak intensities of the 100% standard (taken from a database of mineral standards) with those in the mixture (Cressey and Schofield 1996). The standard pattern was then decreased by the appropriate factor and effectively stripped out of the original sample. As the patterns (peaks plus background) for each Fe-containing phase were subtracted, the residual background (related to the amount of Fe present in each remaining phase) was reduced in intensity and the sum of identified phases eventually totalled 100% (i.e., 100% of the pattern can be fitted if all phases are correctly identified and correctly proportioned). The percentages of phases obtained by this technique are "percentages of fit." Low absorbers such as forsterite-rich olivines yield lower "percentages of fit" than their actual wt% present in the sample (the result of attenuation of X-rays owing to absorption by the bulk matrix that contains high absorber phases such as fayalite-rich olivine, troilite and Fe-Ni metal). Conversely high absorbers yield a higher "percentage of fit" than actual. The correction for absorption was carried out using the "percentage of fit" and the mass absorption coefficient (μ/ρ) which is different for each mineral in a mixture (Cressey and Schofield 1996). Weight proportions can be converted to volume proportions using the density (ρ) for each pure phase identified. The error on the corrected wt% figures is estimated to be ~2 wt%. However, the values are shown and quoted to one decimal place in order to preserve them before performing other calculations and avoid additional errors by rounding the data too early.

A specific problem was encountered for Fe-Ni metal. The metal, being denser and composed of larger grains, tends to sink into the less dense powder during sample preparation so the X-rays "see" a less than representative proportion of metal. To overcome this problem the metal was magnetically separated and weighed after the XRD experiment. The silicate and sulfide phase proportions (determined from XRD experiment) were then re-proportioned to sum 100-metal% (found by weighing the magnetic separate).

Meteorite Samples

The UOCs are subdivided from 3.0 to 3.9, with increasing gradational metamorphism, on the basis of thermoluminescence sensitivity and olivine composition (Sears et al. 1980). Only 4% of the known ordinary chondrites are unequilibrated (Grady 2000) and only a small proportion of these are recent falls large enough to permit a detailed mineralogical study. In order to analyze an entire series of UOCs from 3.1 to 3.9, twenty one UOCs collected in the Antarctic were chosen for this study (Table 1). In order to test if Antarctic weathering affected trends observed in the series, fourteen recent falls were also analyzed. These were Semarkona, Bishunpur, Bovedy, Chainpur, Manych, Hallingeberg, Sharps, Tieschitz, Ngawi, Parnallee, Ceniceros,

Table 1. Mössbauer spectroscopy "percentage of fit" data for unequilibrated ordinary chondrites, divided into finds (Antarctic) and falls. Errors on the spectral areas are given in the text. The quadrupole splitting Δ value in mm/s of olivine for each meteorite is also shown and has an error of ± 0.02 mm/s.

Meteorite	Petrol. type	Olivine%	Pyroxene%	ParaFe^{3+}%[a]	Troilite%	Fe-Ni metal%	Magnetite%	Olivine Δ mm/s
LEW 86134	L3.0	30.4	11.2	36.7	12.9	–	8.8	2.91
LEW 86018	L3.1	44.1	13.1	24.0	16.3	2.5	–	2.91
ALH A77176	L3.2	37.6	15.3	27.0	13.8	6.3	–	2.91
ALH 83010	L3.3	48.2	20.8	10.7	20.3	–	–	2.92
GRO 95658	LL3.3	51.5	16.3	22.4	9.8	–	–	2.92
WSG 95300	H3.3	43.0	12.5	18.3	8.7	17.5	–	2.90
ALH 84126	LL3.4	51.1	16.7	11.4	14.3	6.5	–	2.93
LEW 88121	H3.4	36.0	12.3	30.9	12.1	8.7	–	2.93
ALH A77260	L3.5	38.5	11.0	24.9	16.7	8.9	–	2.93
LEW 88336	LL3.5	56.7	17.1	12.4	13.8	–	–	2.91
ALH A81024	L3.6	26.5	8.6	48.1	16.8	–	–	2.93
DAV 92302	LL3.6	56.3	23.4	6.4	13.9	–	–	2.93
QUE 93030	H3.6	37.1	17.9	14.8	10.5	19.7	–	2.94
ALH 90411	L3.7	56.1	15.6	8.7	17.3	2.3	–	2.93
EET 83213	LL3.7	59.9	19.6	6.9	13.6	–	–	2.94
GRA 95208	H3.7	45.7	21.9	13.4	15.9	3.1	–	2.94
ALH 84086	LL3.8	59.5	24.1	3.1	13.3	–	–	2.93
ALH 85045	L3.8	54.4	17.6	6.8	14.8	6.4	–	2.93
GRA 98050	H3.8	32.1	16.5	27.1	15.6	8.7	–	2.94
ALH 84205	L3.9	50.9	21.7	7.7	16.4	3.3	–	2.93
EET 87778	H3.9	31.3	23.6	20.9	16.7	7.5	–	2.95
Bovedy	L3	50.9	25.2	5.1	15.4	–	3.4	2.91
Semarkona	LL3.0	33.8	30.7	20.5	10.6	–	4.4	2.92
Bishunpur	LL3.1	41.9	16.0	9.7	17.1	15.3	–	2.89
Chainpur	LL3.4	45.4	12.7	13.0	19.9	7.6	1.4	2.88
Manych	LL3.4	50.8	30.7	–	18.5	–	–	2.88
Hallingeberg	L3.4	39.6	16.4	5.2	19.9	19.8	–	2.88
Sharps	H3.4	34.2	14.2	10.1	13.1	28.5	–	2.88
Tieschitz	H3.6	59.0	16.1	4.6	11.7	8.6	–	2.90
Ngawi	LL3.6	49.7	20.2	13.8	11.7	–	4.6	2.91
Parnallee	LL3.6	38.0	16.4	11.8	24.1	7.2	2.5	2.96
Ceniceros	H3.7	42.3	15.3	14.0	20.6	7.8	–	2.92
Mezö-Madaras	L3.7	44.5	15.4	11.4	15.3	9.6	3.8	2.91
Gorlovka	H3.7	33.4	20.1	–	17.5	29	–	2.89
Dhajala	H3.8	39.2	25.5	3.4	14.3	17.6	–	2.94

[a]ParaFe^{3+} is a paramagnetic Fe^{3+} phase, probably an Fe-bearing phyllosilicate.

Mezö-Madaras, Gorlovka, and Dhajala. All samples were analyzed by Mössbauer spectroscopy.

A more limited set of six of the UOCs and three EOC recent falls (Muddoor, Soko-Banja, and Kernouve) was chosen for study by XRD.

RESULTS AND DISCUSSION

Mineralogy Identified by Mössbauer Spectroscopy and XRD

Mössbauer spectra for two UOCs are shown in Fig. 1, an Antarctic find, LEW 88121 (H3.4) and a non-Antarctic fall, Bishunpur (LL3.1). The components containing Fe are fitted using three doublets representing paramagnetic Fe in olivine, low-Ca pyroxene and phyllosilicate, and two sextets representing ferromagnetic Fe in troilite and Fe-Ni metal. Integrating the areas underneath the fitted curves yields the proportion of the total Fe contained in that phase. These are the "percentage of fit" values given above each spectrum. Table 1 shows all the minerals identified in the ordinary chondrites analyzed by Mössbauer spectroscopy as "percentages of fit," not as modal wt% values. The average errors on the spectral area percentages are 1.4, 5.6, 8.2, 9.3, and 12.8% for Fe in Fe^{3+}-rich phases, olivine, pyroxene, troilite, and Fe-Ni metal, respectively (Bland et al. 1997). We are using Mössbauer spectroscopy primarily as a mineral identification tool and XRD to provide quantitative values.

In some case the "percentage of fit" values can be converted to wt% values. Silicates (olivine, pyroxene, and

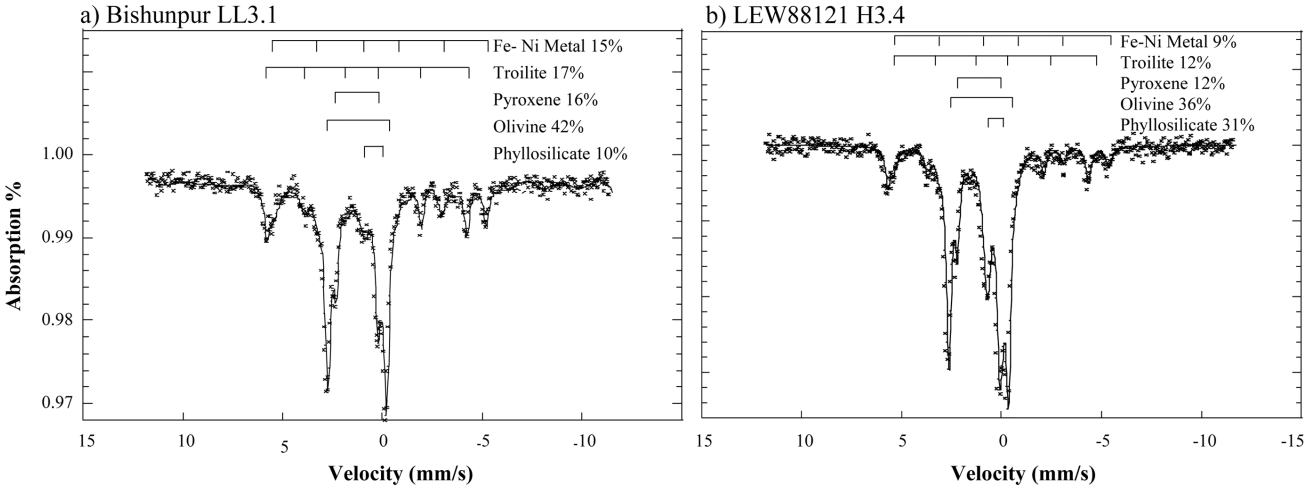

Fig. 1. Mössbauer spectra of a) Bishunpur, LL3.1 and b) LEW 88121, H3.4. Shown are the fitted spectra composed of two sextets (Fe-Ni metal and troilite) and three doublets (olivine, pyroxene, and phyllosilicate). To a first approximation, the areas underneath the fitted curves represent the proportion of the total Fe contained in that phase. The "percentage of fit" values for each mineral phase are given above the spectra and the errors are given in the text. Note that the Antarctic find (b) has a larger proportion of terrestrially-derived phyllosilicate.

clay) have highly heterogeneous compositions in UOCs. This means that it is not possible to accurately calculate their Fe content by stoichiometric means. Troilite and magnetite have reasonably constant stoichiometries: the percentage of Fe in troilite is 63.5% and in magnetite, 72.3%. Bland et al. (1997) have used this to calculate wt% magnetite in carbonaceous chondrites.

Calculating for troilite,

wt% troilite in meteorite =
(Mössbauer % age of fit assigned to troilite ×
total wt% Fe in meteorite) / % age of Fe in troilite (1)

e.g., for Chainpur:

$$\frac{19.9 \times 19.78}{63.5} = 6.2 \text{ wt\%} \quad (2)$$

This is comparable to the 6.4% FeS measured by Jarosewich (1990). All of the converted wt% values for troilite and magnetite are shown in Table 2. The average difference between the wt% estimate derived from Mössbauer data and those obtained by Jarosewich (1990) is 1.2 wt%.

Figure 2 shows XRD patterns for Bishunpur and Kernouve (H6) with the experimental pattern of the bulk sample alongside the calculated pattern, which is the composite of all standard phases believed to be present in the sample. The residual pattern is the experimental minus the calculated pattern and should be a flat line when all phases are accounted for. Narrower and more intense peaks were observed in Kernouve reflecting this meteorite's enhanced equilibration. Some peaks remained in the residual pattern owing to enhanced reflections from some larger crystals in either the standard or sample powder mounts. Cressey and Schofield (1996) showed that the presence of residual peaks in the final pattern has no effect on the final quantification. Consequently these peaks can be disregarded. Table 3 shows the XRD-quantified modal mineralogy of nine ordinary chondrites. The error on these figures is ~±2 wt%.

As the total fluorescence background is proportional to the amount of Fe in the sample and is equivalent to the sum of the fluorescent backgrounds from each component phase, it is possible to use the fluorescence background to aid the fitting procedure. Then, by using a knowledge of the phase proportions and their Fe weight fractions, the total wt% of Fe can be calculated. All but one meteorite analyzed is within 2.8% of its published total Fe wt% value. These values are given in Table 3. This gives us additional confidence that we are obtaining a realistic mineral assemblage for each meteorite and implies that the XRD results are directly comparable to those obtained by Mössbauer spectroscopy.

Comparisons with Bulk Chemistry

An effective test of the validity of the modal mineralogical assessment is provided by comparing predicted bulk chemistry, derived from our phase proportions, to literature bulk chemistry for each sample. Therefore the mineralogical data obtained from XRD analysis is converted to elemental values in order to make comparisons between our modal data and the published bulk chemistry for ordinary chondrites (Jarosewich 1990; Easton and Elliot 1977 [for Soko-Banja]; Hutchison et al. 1981 [for Kernouve]). Literature bulk chemical data are available for all the chondrites analyzed except Muddoor. The XRD modal data were converted to bulk chemistry using the best-fit standards available. An average augite composition of $Mg_1,Ca_{0.8},Fe_{0.2}Si_2O_6$ was assumed (Brearley and Jones 1998) and anorthite was taken in each case to be pure $CaAl_2Si_2O_8$

Table 2. Mössbauer spectral areas of troilite and magnetite in ordinary chondrites converted to wt% values as described in the text. Comparisons are made where possible with wt% FeS values from Jarosewich (1990).

				Troilite		Magnetite	
		Total Fe (wt%)[a]	Mössbauer "% age of fit"	Calculated wt%	Jarosewich wt%	Mössbauer "% age of fit"	Calculated wt%
Bovedy	L3	22.48	15.4	5.5	6.5	3.4	0.3
Semarkona	LL3.0	19.09	10.6	3.2	5.3	4.4	0.2
Bishunpur	LL3.1	19.97	17.1	5.4	6.5	–	–
ALH A77176	L3.2	20.2	13.8	4.4	–	–	–
Chainpur	LL3.4	19.78	19.9	6.2	6.4	1.4	0.1
ALH A77260	L3.5	20.39	16.7	5.4	3.4	–	–
Manych	LL3.4	19.11	18.5	5.6	8.4	–	–
Hallingeberg	L3.4	21.97	19.9	6.9	6.6	–	–
Sharps	H3.4	26.26	–	–		–	–
Tieschitz	H3.6	25.13	11.7	4.6	5.3	–	–
ALH A81024	L3.6	24.2	16.8	6.4	–	–	–
Parnallee	LL3.6	18.29	24.1	6.9	–	2.5	0.2
Mezö-Madaras	L3.7	21.6	15.3	5.2	6.0	3.8	0.3
Dhajala	H3.8	27.1	14.3	6.1	5.1	–	–

[a]Total Fe wt% values are taken from Jarosewich (1990) except Parnallee (Dodd et al. 1967) and ALH A77176 and ALH A81024 (Sears and Hasan 1987).

(no albite was evident in any of the meteorites analyzed). Smectite compositions were from Alexander et al. (1989) for Bishunpur. Kamacite compositions were taken where possible from Rubin (1990) and taenite from Hutchison et al. (1981).

A comparison of the literature data compared with those calculated from our XRD results is portrayed in Fig. 3. The best-fit lines for each meteorite indicate that an almost ideal 1:1 relationship exists between the two data sets. Given that this is a simple conversion and does not take into account the abundances of minor elements (Ti, Cr, Mn, K, P, Co, C) which account for up to up to ~2% of the samples, and that some of the mineral compositions used are simplistic analogues, the mineralogical data obtained by XRD do appear to yield a good approximation to bulk chemical analyses. In several of the meteorites analyzed the abundance of Fe is slightly overestimated by the XRD technique (in Dhajala and Kernouve it is almost identical to the published chemical analyses). This may be owing to an overestimation of the weighed amount of metallic iron. This is more likely to be an issue with the unequilibrated L and LL chondrites which contain finer and more dispersed Fe-Ni metal particles.

The Mg/Si ratio of chondrites is used to distinguish between the ordinary, carbonaceous and enstatite chondrites, and is considered to be an approximately constant value within meteorite groups. The Mg/Si ratio of ordinary chondrites ranges between 0.78 and 0.85 (Dodd 1981). Using the bulk chemistry data calculated from XRD mineralogy, we obtain Mg/Si ratios ranging between 0.77 and 1.08. Only three meteorites have ratios that are significantly different from those expected from literature bulk chemistry. We note that by changing the XRD-derived proportions of individual silicate phases by an average of ≤2% (i.e., within error on our phase proportions) it is possible to match the expected Mg/Si ratio for each chondrite.

The fact that the bulk chemistry obtained from the mineralogical assessments made by XRD is close to the published bulk chemical data suggests that our XRD experimental and fitting procedure provides a reasonable approximation of the actual modal mineralogy of each sample.

Phyllosilicates

The presence of phyllosilicate, or clay, in the bulk samples was difficult to determine by XRD alone because of its generally low proportion, poor crystallinity and fine particle size. XRD was carried out at a high incidence angle to obtain better resolution for ferromagnesian silicates. Clays have diagnostic peaks at low angles of 2θ and consequently were not observed. Instead higher angle, diffuse clay peaks were used for quantification (an advantage being that these peaks are unlikely to be produced by preferred orientation) (Batchelder and Cressey 1998). Low angle diffraction analysis was carried out to try to further identify the phyllosilicate species. Poor crystallinity and fine grain size rendered the peaks as two overlapping, diffuse, low intensity bumps at 4° and 8.8° 2θ in the most equilibrated chondrites studied, indicating a composition that is almost certainly a mixed layer clay containing smectite and illite.

In addition, Mössbauer spectroscopy identified a paramagnetic ferric phase in all the ordinary chondrites sampled. Ferric-bearing minerals that may be present in chondrites include phyllosilicates, maghemite, goethite, and ferrihydrite. The ferric proportion that may be contained in pyroxene is too small to be of significance. Phyllosilicates are known to be present in several ordinary chondrites (e.g., Hutchison et al. 1987; Alexander et al. 1989; Grossman et al. 2000) and are the most likely source of the paramagnetic Fe^{3+} phase observed in the Mössbauer spectra. If other ferric-bearing phases exist, they must be present at abundances <1–2 wt%.

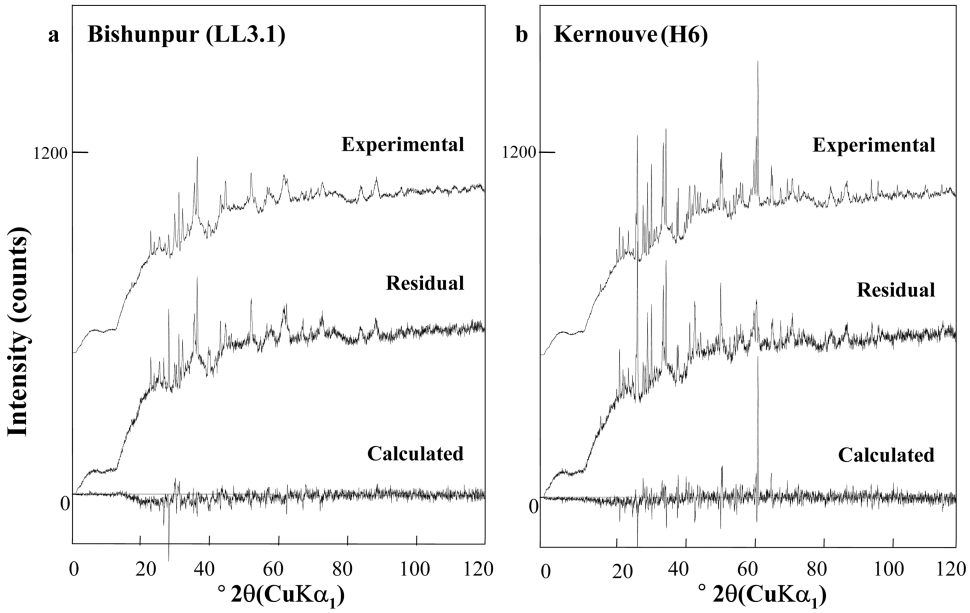

Fig. 2. X-ray diffraction patterns for a) Bishunpur, LL3.1 and b) Kernouve, H6. Shown are the experimental patterns of the bulk samples, the calculated composites of all standard phases believed to be present and the residual patterns (experimental minus calculated). The experimental patterns have been offset by 500 counts on the y-axis. Note the narrower, more intense peaks in the equilibrated Kernouve. Some peaks remain in the residual pattern owing to enhanced, single crystal reflections; these peaks can be disregarded and they do not affect the bulk quantification results.

Bishunpur was found to contain a large proportion of a phyllosilicate phase. This was observed both by the characteristic peaks in the XRD pattern and by the presence of a paramagnetic Fe^{3+} phase in the Mössbauer spectrum. Alexander et al. (1989) described the presence of a smectite phase in Bishunpur by using transmission electron microscopy (TEM) and give a range of measured compositions. Using a chemical formula midway between the compositional ranges given by Alexander et al. (1989), our XRD analysis is consistent with Bishunpur containing 19.9 wt% smectite. The same chemical formula was used to convert the Mössbauer values for the paramagnetic Fe^{3+} phase to wt% values. Using this method the proportions of smectite in Bishunpur was found to be 20.4 wt%.

Taking the same approach for Semarkona, using the smectite composition reported by Hutchison et al. (1987) and the Mössbauer "percentage of fit" value of 20.5%, we find Semarkona to contain ~15.4 wt% smectite.

That aqueous alteration products are not considered to be abundant in Bishunpur and Semarkona based on petrographic studies does not preclude their presence as a major component within these meteorites. Numerous studies of incipient alteration in terrestrial ferromagnesian silicates have described the pervasive development of narrow sub-parallel channels, a few tens of nanometer wide, filled with Fe-rich clays and Fe oxyhydroxides. Such channels are found throughout these silicates, their overall orientation controlled by the host mineral crystal structure (Eggleton 1984; Smith et al. 1987; Banfield et al. 1990; Hochella and Banfield 1995). As alteration proceeds, the silicate begins to part along this preferred orientation. This type of texture, where smectite structure follows the crystallographic orientation of the precursor silicate, is known as a topotactic alteration, and appears to be almost ubiquitous in the incipient alteration of olivine and pyroxene (Eggleton 1984; Smith et al. 1987; Banfield et al. 1990; Hochella and Banfield 1995). Bland et al. (2000) have observed a similar feature in the alteration of meteoritic silicates. TEM analyses indicated a strong control on incipient alteration by crystal structure of the silicate, demonstrated by topotactic clays on both olivine and pyroxene. In this case the overall orientation of the channels appeared to be controlled by irregular fractures, defects, or sub-domains within the silicate, created during impact-related shock events.

In both terrestrial and extraterrestrial samples, although the channels themselves may only be a few tens of nanometers wide, their pervasive development means that the total volume they occupy may be quite large. Despite this, macroscopic effects, visible by SEM and optical microscopy, will not be visible until the silicate begins to part, whether along a crystallographic orientation or on sub-domains defined by a shock event. This alteration will, however, be "visible" to both Mössbauer spectroscopy and X-ray diffraction. The fact that both techniques, one using short range order and the other using long-range order, detect approximately the same abundance of these alteration products, suggests that they are indeed a major component within these meteorites.

Table 3. X-ray diffraction data for six UOC and three EOC falls.

	Mineral phase	XRD % fit[a]	μ/ρ[b]	Weight fraction Fe	wt% XRD sample[c]	wt% actual[d]	Total Fe% (lit.)[e]	Total Fe% (calc.)[f]
Bishunpur LL3.1								
	Forsterite 100	5	32.2	0	10.7	9.4	20.0	22.3
	Forsterite 80	18	71.3	0.146	17.4	15.2		
	Forsterite 60	9	104.5	0.269	5.9	5.2		
	Forsterite 50	4	119.2	0.324	2.3	2.0		
	Fayalite 100	5	179.3	0.548	1.9	1.7		
	Augite	5	66.5	0.051	5.2	4.5		
	Enstatite 98	14	36.4	0.011	26.5	23.2		
	Kamacite	5	304.4	0.925	1.1	7.8		
	Taenite	3	225.0	0.700	0.9	6.3		
	Troilite	12	146.0	0.635	5.7	5.0		
	Smectite	20	61.4	0.095	22.4	19.7		
Manych LL3.4								
	Forsterite 100	6	32.2	0	15.4	14.6	20.8	21.7
	Forsterite 80	20	71.3	0.146	23.2	22.0		
	Forsterite 60	23	104.5	0.269	18.2	17.3		
	Forsterite 25	10	151.8	0.446	5.4	5.2		
	Augite	11	66.5	0.051	12.4	11.8		
	Enstatite 83	10	58.2	0.011	15.6	14.9		
	Kamacite	3	304.4	0.935	0.8	5.6		
	Troilite	14	146.0	0.635	7.9	7.5		
	Magnetite	3	223.3	0.724	1.1	1.1		
Soko-Banja LL4								
	Forsterite 80	20	71.3	0.146	24.0	22.3	19.9	22.7
	Forsterite60	49	104.5	0.269	40.1	37.2		
	Augite	8	66.5	0.051	10.3	9.6		
	Enstatite 77	4	66.1	0.122	5.2	4.8		
	Kamacite	2	304.4	0.929	0.6	3.5		
	Taenite	2	225.0	0.700	0.8	4.8		
	Troilite	5	146.0	0.635	2.9	2.7		
	Anorthite	10	52.7	0	16.1	15.1		
Hallingeberg L3.4								
	Fosterite 80	20	71.3	0.146	25.4	23.7	22.0	25.8
	Fosterite 60	18	104.5	0.269	15.6	14.5		
	Fosterite 50	10	119.2	0.324	7.6	7.1		
	Fosterite 25	6	151.8	0.446	3.6	3.3		
	Augite	14	66.5	0.051	19.1	17.8		
	Enstatite 83	6	58.2	0.092	9.3	8.7		
	Anorthite	5	52.7	0	8.7	8.0		
	Kamacite	6	304.4	0.95	1.8	6.5		
	Taenite	2	225.0	0.700	0.8	2.9		
	Troilite	13	146.0	0.635	8.1	7.5		
Mezö-Madaras L3.7								
	Forsterite 80	28	71.3	0.146	33.3	30.9	21.6	23.1
	Forsterite 60	25	104.5	0.269	20.4	18.8		
	Augite	8	66.5	0.051	10.2	9.5		
	Enstatite 83	13	58.2	0.011	19.0	17.6		
	Kamacite	5	304.4	0.950	1.4	4.9		
	Taenite	4	225.0	0.700	1.6	5.3		
	Troilite	13	146.0	0.635	7.6	7.0		
	Anorthite	4	52.7	0	6.5	6.0		
Muddoor L5								
	Forsterite 80	36	71.3	0.146	40.7	36.8	Unknown	25.1

Table 3. *Continued.* X-ray diffraction data for six UOC and three EOC falls.

	Mineral phase	XRD % fit[a]	μ/ρ[b]	Weight fraction Fe	wt% XRD sample[c]	wt% actual[d]	Total Fe% (lit.)[e]	Total Fe% (calc.)[f]
	Forsterite 80	13	104.5	0.269	10.0	9.0		
	Augite	12	66.5	0.051	14.5	13.1		
	Enstatite	10	58.2	0.092	13.9	12.6		
	Kamacite	7	304.4	0.950	1.9	11.3		
	Anorthite	7	52.7	0	10.7	9.7		
	Troilite	15	146.0	0.635	8.3	7.5		
Sharps H3.4								
	Forsterite 100	5	32.2	0	12.6	10.6	26.3	28.2
	Forsterite 88	6	56.4	0.090	8.7	7.3		
	Forsterite 80	18	71.3	0.146	20.7	17.3		
	Forsterite 60	18	104.5	0.269	14.1	11.8		
	Forsterite 50	8	119.2	0.324	5.5	4.6		
	Augite	9	66.5	0.051	11.1	9.3		
	Enstatite 86	11	53.3	0.074	16.9	14.2		
	Kamacite	7	304.4	0.921	1.9	7.9		
	Taenite	8	225.0	0.700	2.9	12.3		
	Troilite	10	146.0	0.635	5.6	4.7		
Dhajala H3.8								
	Forsterite 88	20	56.4	0.090	26.8	22.2	27.1	27.3
	Forsterite 80	25	71.3	0.146	26.5	21.9		
	Augite	11	66.5	0.051	12.5	10.4		
	Enstatite 89	10	50.0	0.062	15.2	12.6		
	Kamacite	8	304.4	0.924	2.0	10.2		
	Taenite	6	225.0	0.700	2.0	10.4		
	Troilite	15	146.0	0.635	7.8	6.4		
	Anorthite	5	52.7	0	7.2	5.9		
Kernouve H6								
	Forsterite 88	19	56.4	0.090	25.2	20.3	28.8	27.5
	Forsterite 80	18	71.3	0.146	20.0	16.1		
	Anorthite	10	52.7	0	14.2	11.4		
	Enstatite 83	22	57.6	0.053	28.6	23.0		
	Kamacite	12	284.1	0.924	3.2	13.5		
	Taenite	7	200.1	0.604	2.6	10.7		
	Troilite	12	146.0	0.635	6.2	5.0		

[a]Raw fit data before any corrections made.
[b]Mass absorption coefficient (linear absorption coefficient/density).
[c]Weight percent of the sample after correction for absorption and before correction for Fe-Ni metal, ±2 wt%.
[d] Final weight percent values for mineral phases after correcting for Fe-Ni metal.
[e]Total Fe weight percent (Jarosewich 1990).
[f]Total Fe weight percent as calculated using final weight percent values and weight fraction of Fe in each mineral phase.

Oxides

Magnetite is also difficult to identify by XRD alone owing to masking of its characteristic peaks by those of olivine, however it is extremely distinctive in Mössbauer spectra. In the sampled analyses, magnetite was predominantly found in the most unequilibrated of LL chondrites and in some L UOCs.

Chromite is present in some UOCs in very small proportions (Huss et al. 1981). In XRD, its peak position is similar to magnetite and would be masked by olivine, however no evidence of chromite was found in any of the Mössbauer spectra. It is likely that any chromite present is not detectable by the methods used in this study owing to its presence at such low abundance.

Olivine and Pyroxene

Both techniques identified olivine and pyroxene. The UOCs contain a heterogeneous mixture of olivine compositions from pure forsterite to pure fayalite (Bishunpur contains both end-members of the olivine solid solution series). Compositions were found by XRD to homogenize to between Fo_{80} and Fo_{60} with equilibration, depending on the class of ordinary chondrite. Exact olivine compositions of EOCs are known from electron microprobe analysis (e.g.,

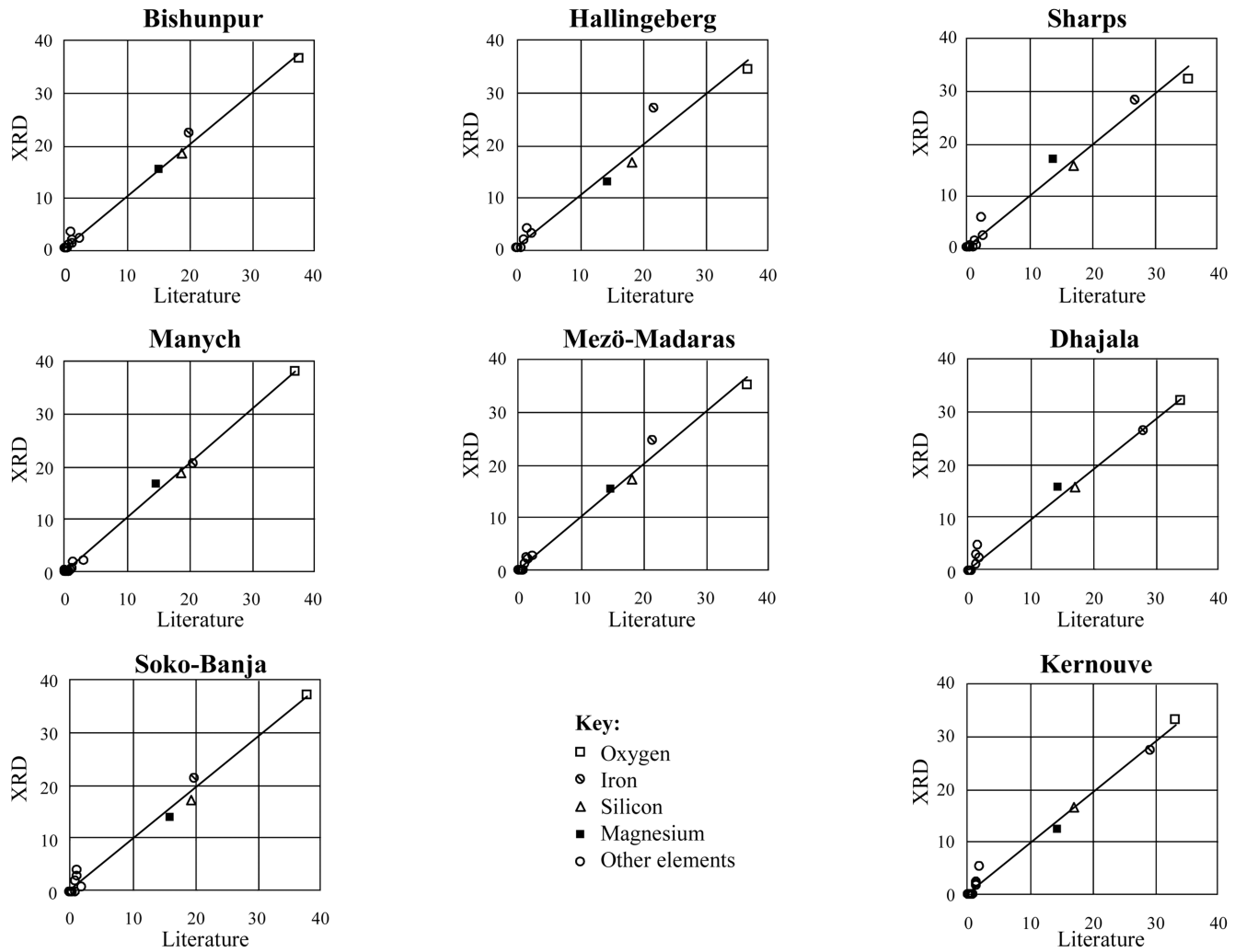

Fig. 3. Graphs showing variation in single element data obtained from the literature (Jarosewich 1990) compared with that calculated from our XRD-derived data. A best-fit line is drawn through the data for each meteorite (the range of R2 values is from 0.97 to 0.99). An almost ideal 1:1 relationship exists between the data sets indicating that the chemical compositions derived from the XRD mineralogy are very close to those expected from the literature values.

Dodd 1981). Our technique cannot yet isolate these exact values as we do not have a sufficiently wide compositional spread of olivine standards, only a limited number of standards in 10 mol% intervals. However, for quantification purposes we can quantify the proportions of olivine present in the sample of an approximately similar composition. With increased numbers of silicate standards we will be able to improve our XRD fitting procedure for unequilibrated chondrites.

Sulfide and Metal

Troilite was observed by both techniques in all of the samples analyzed. No evidence was found for the presence of any other sulfide, e.g., pyrrhotite or pentlandite, indicating that if they are present they are at abundances <1–2 wt%. Troilite abundances are known to remain approximately constant in ordinary chondrites of all petrologic types (Jarosewich 1990). Table 2 shows that the proportions of troilite obtained by Mössbauer spectroscopy in UOC falls are relatively constant, between 3–7 wt% and are within 2.5 wt% of the XRD values.

Metallic iron was clearly detected in the Mössbauer spectra and XRD patterns of all H chondrites and some L and LL chondrites. XRD also allowed for the differentiation between kamacite and taenite and allocation of weight proportions to each polymorph. LL chondrites contain dispersed, fine-grained Fe-Ni metal particles which may have attracted fine silicate particles as they were extracted by magnetic separation. However, the magnetic phases removed by magnetic separation were analyzed by XRD and found to have little or no silicate/sulfide contamination. Bishunpur appears to have a substantially larger proportion (14.1 wt%) of Fe-Ni metal than expected for an LL chondrite. From Table 1 it can be seen that Mössbauer spectroscopy also

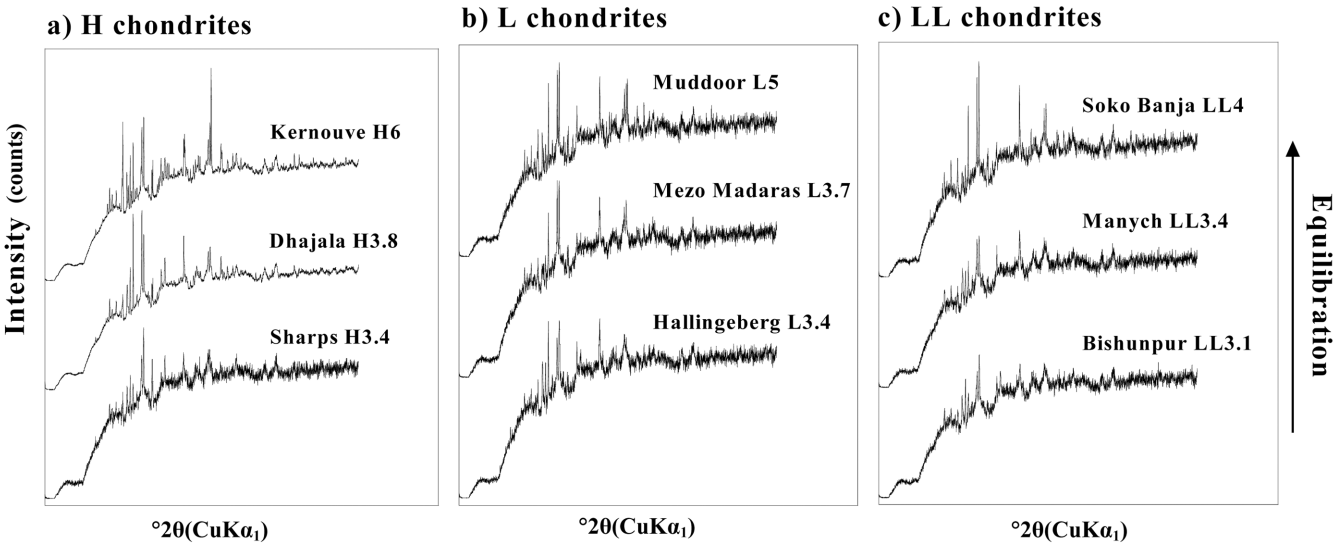

Fig. 4. Experimental X-ray diffraction patterns for a) H, b) L, and c) LL chondrites stacked in order of increasing equilibration. (The patterns are offset by 500 counts along the y-axis.) Note that diffraction peaks, which are dominantly of olivine, appear more intense with equilibration; this is because the olivines have become more singular in composition upon recrystallization and give enhanced reflections.

shows this meteorite to have a large proportion of Fe-Ni metal (15.3 wt%).

Mineralogical Trends

Experimental XRD patterns for the ordinary chondrites analyzed are portrayed in Fig. 4, showing that peaks become narrower and more intense as crystallinity increases and compositions homogenize with equilibration. In addition, both Mössbauer spectroscopy and X-ray diffraction data showed systematic mineralogical changes with metamorphism in both the abundance and composition of phases.

Figure 5a uses stacked columns to represent the changing mineralogy (observed by Mössbauer spectroscopy) with petrologic type in the Antarctic LL UOCs. As previously discussed it is possible to convert Mössbauer data to wt% values (Bland et al. 1998), but here Mössbauer spectroscopy "percentage of fit" data are compared for different chondrites. (The comparison is internally consistent and so observed trends remain valid.)

All of the samples contain a paramagnetic phase indicative of a ferric-bearing phyllosilicate. This phase clearly decreases in abundance with metamorphism, an inverse relationship to that observed for both olivine and pyroxene. The suggestion is that dehydration of phyllosilicate occurred with progressive metamorphism to produce ferromagnesian silicates.

Ferric Fe is indicative of oxidative weathering in a hydrous environment (Burns 1993). It is important to be aware that the Antarctic meteorites are all finds and have as a result been terrestrially weathered to varying degrees (Gooding 1986). The trends observed in Fig. 5a were confirmed by comparison with UOC falls exposed to less terrestrial alteration. Fig. 5b shows all UOC LL falls analyzed by Mössbauer spectroscopy along with data for several EOC falls. The UOC falls show the same inverse relationship between ferromagnesian silicates and phyllosilicates, as seen in the Antarctic finds. The mineralogy of the LL6 chondrites is uniform in comparison. Magnetite is observed in all UOC falls (except Bishunpur) but is not evident in the Antarctic finds. If this absence is the result of terrestrial, Antarctic weathering, then it is a surprising result given the stability of magnetite in terrestrial surface environments and its resistance to alteration.

The fact that clear trends in the silicate mineralogy are observed with increasing equilibration, while troilite abundances remain constant, and that the same trends are observed in analyses of falls, gives us confidence in the Antarctic meteorite data. It suggests that terrestrial alteration is a minor component and most of the trends we observe are the result of pre-terrestrial alteration of ordinary chondrites.

Antarctic L chondrites contain larger proportions of phyllosilicate than LLs, and one L3.6 (ALH A81024) has an inordinately large amount of (probably) terrestrially-derived clay. However, the same overall trend of decreasing proportions of phyllosilicate and increasing proportions of ferromagnesian silicates with equilibration is observed in both Antarctic L finds and L falls. H chondrites show irregular variations in phyllosilicate content and variable amounts of Fe-Ni metal. Any systematic changes in silicate mineralogy are indistinct. This may be owing to their increased vulnerability to terrestrial alteration (Bland et al. 1998).

Krot et al. (1997) have shown that fayalitic olivine in CV3 chondrites could be formed by aqueous alteration of

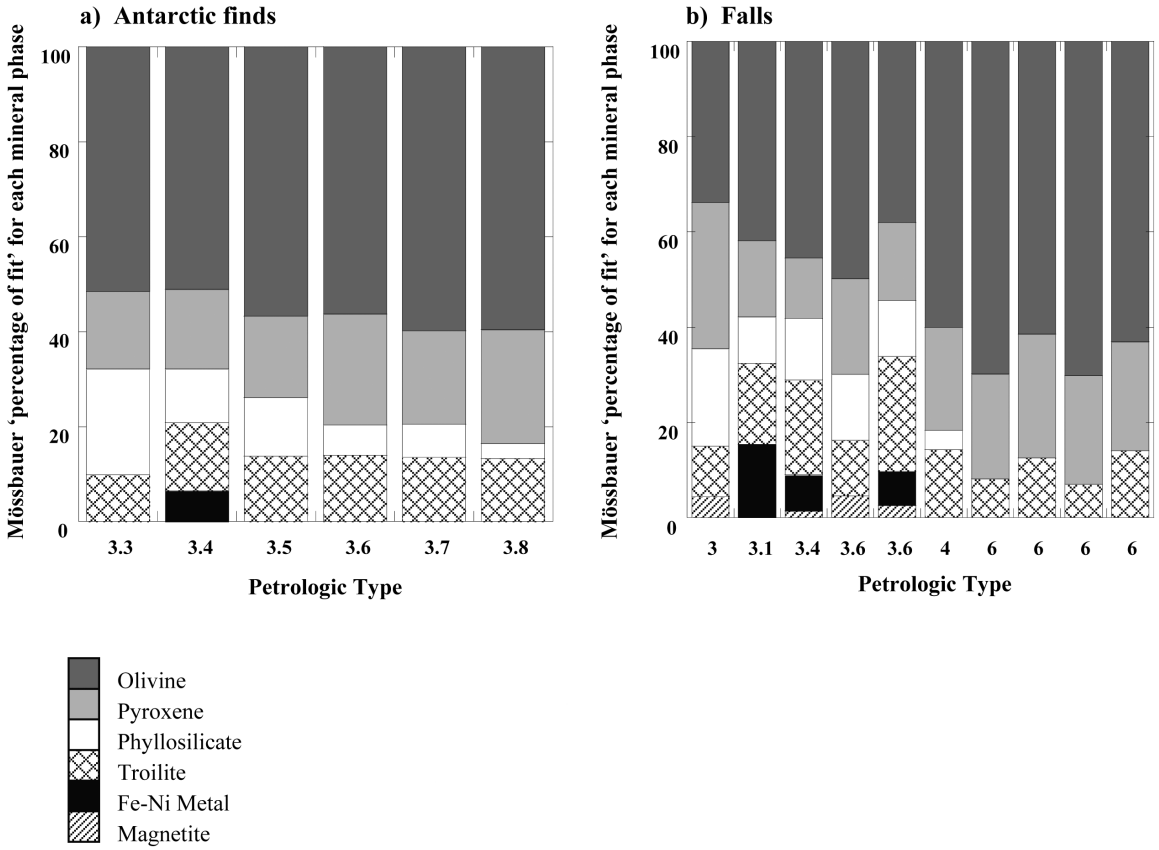

Fig. 5. Changing mineralogy with petrologic types for LL chondrites as shown by Mössbauer spectroscopy for a) Antarctic finds and b) falls. Mössbauer "percentage of fit" data can be roughly approximated to Fe-containing mineral proportions. Both finds and falls show decreasing proportions of phyllosilicate and increasing proportions of ferromagnesian silicates with progressive metamorphism (increasing petrologic type) throughout the UOCs. These trends are not visible in the most equilibrated falls.

ferromagnesian silicates and subsequent dehydration of phyllosilicates within the parent body. Although ordinary chondrites are substantially less altered than carbonaceous chondrites, they contain ubiquitous evidence of aqueous alteration in the form of "bleached chondrules" (Grossman et al. 2000). We suggest that the ordinary chondrites may have undergone a similar progressive process of fluid-assisted metamorphism as described for the CV3s (Krot et al. 1997).

Analysis of modal mineralogy derived from XRD analysis shows similar trends to those observed by Mössbauer spectroscopy. Figure 6a shows the changing mineralogy of three LL chondrites where the large proportion of phyllosilicate in the less equilibrated samples is very obvious. As already observed from the Mössbauer data, the proportions of ferromagnesian silicate increase with metamorphism.

Feldspar, not being an Fe-containing mineral, is not identified by Mössbauer spectroscopy. It is observed predominantly as anorthite in XRD patterns of UOCs from petrologic type 3.4. This trend is consistent with the observations of Huss et al. (1981) and Sears et al. (1982). In their assessment of the anhydrous mineralogy of ordinary chondrites, McSween et al. (1991) were unable to obtain accurate normative data for feldspar, finding it more abundant and anorthite-rich than actual feldspar. Figure 6b shows the normative values of McSween et al. (1991) for the same two UOCs as Fig. 6a but with Greenwell Springs replacing Soko Banja, as it was the only LL4 examined in that study. The proportion of normative olivine is seen to rise with increasing equilibration but only at the expense of normative pyroxene. The three chondrites in the McSween et al. (1991) study show constant amounts of feldspar, troilite, and Fe-Ni metal.

There is clearly a large and fundamental variation between modal and normative mineralogy which goes beyond the "minor differences" suggested by Dodd (1981). We feel that the Mössbauer spectroscopy and X-ray diffraction data are mutually supportive and this allows us to be confident in our assessment of the modal mineralogy of these unequilibrated meteorites.

Mössbauer Parameters and Reduction during Metamorphism

Quadrupole splitting is a parameter obtained by Mössbauer spectroscopy for minerals containing paramagnetic Fe, i.e., olivine, pyroxene, and phyllosilicates in

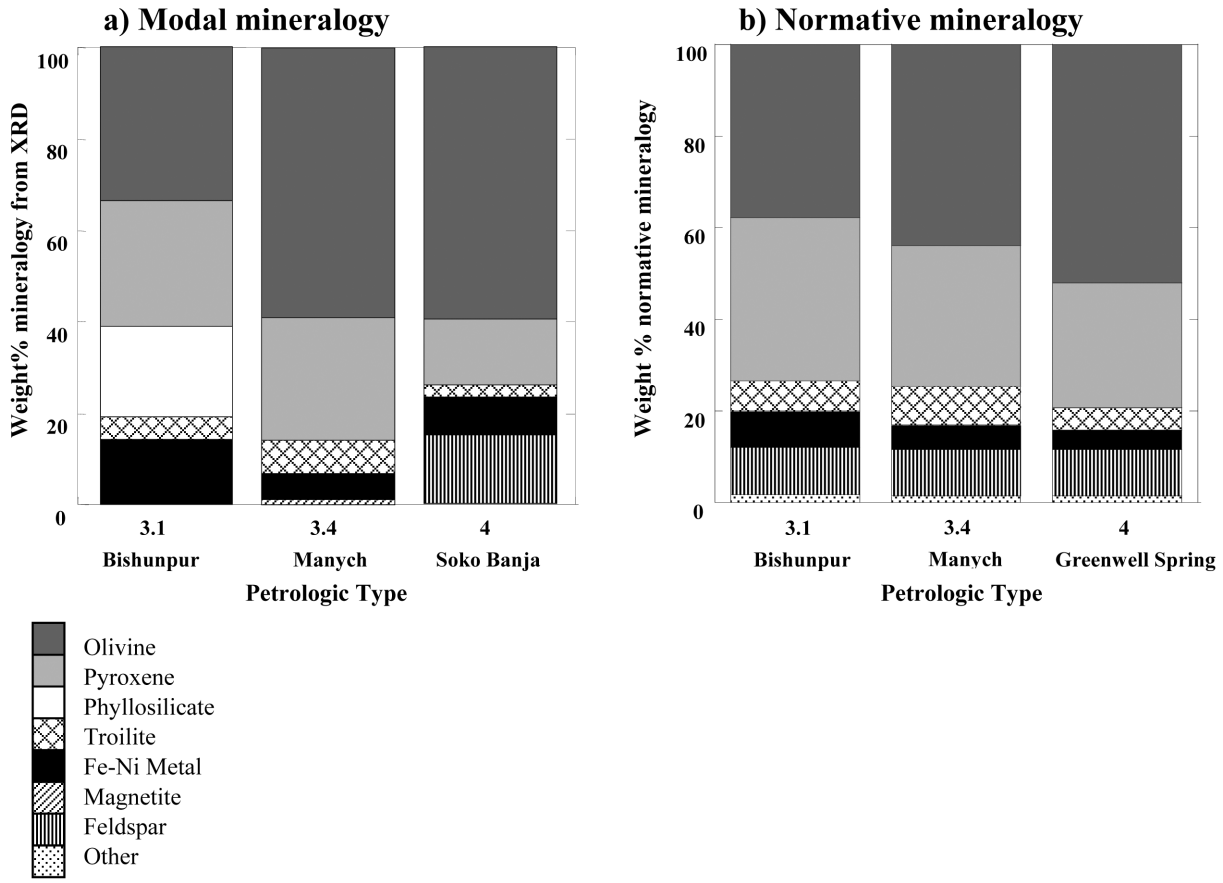

Fig. 6. Changing mineralogy with petrologic types for LL chondrites: a) modal mineralogy for falls by XRD; b) normative mineralogy (McSween et al. 1991). XRD analysis does not identify crystalline feldspar in the most unequilibrated LL chondrites in contrast to the normative mineralogical calculations. Phyllosilicates are identified by XRD but are not included in the anhydrous normative mineralogy investigation.

chondrites. It provides an indication of the symmetry of the bonding environment and local structure around the Fe site. Menzies et al. (2001) showed that quadrupole splitting is correlated with silicate chemistry in EOCs. Fig. 7 shows the relationship between the quadrupole splitting values and forsterite content for synthetic mono-mineralic olivines (Menzies et al. 2001). As discussed by Menzies et al. (2001), it is apparent that quadrupole splitting increases with increasing Mg content. The homogenous olivine in EOCs shows the same correlation. H chondrites, containing silicates with higher Mg contents, have larger values of quadrupole splitting than L and LL chondrites.

UOCs do not possess a single unique olivine composition, so UOC data cannot be presented in the same manner as in Fig. 7. (Quadrupole splitting values for olivine in UOCs are given in Table 1.) We might presume that the measured values of quadrupole splitting represent some average of all the olivine compositions present in a meteorite. Figure 8 shows quadrupole splitting values for bulk olivine in each UOC (falls and Antarctic finds) plotted against the petrologic type. It should be noted that the scale on the x-axis is not a linear one as it is not possible to compare directly UOC and EOC metamorphic grade using one unifying parameter. Feldspar thermoluminescence or percent mean deviation of olivine composition could be used for comparing only the UOCs but neither scale extends into the EOCs. It can be seen that quadrupole splitting increases with petrologic type, i.e., with metamorphism, throughout the UOCs. This trend does not follow into the EOCs and they may in fact show a slight negative correlation.

As quadrupole splitting is a measure of symmetry and order at the Fe site (e.g., Berry 1983), Fig. 8 might suggest that olivine in UOCs has a more ordered structure. This seems at odds with the fact that the olivine in UOCs is highly heterogeneous (van Schmus and Wood 1967). However, as discussed above, Menzies et al. (2001) showed that increasing quadrupole splitting correlates with increasing forsterite content (Fig. 7). By applying this relationship to the UOCs, we would conclude that olivine becomes more forsteritic with increasing petrologic type, i.e., that Fe is lost from olivine during metamorphism.

Previous work has shown that the matrix of ordinary chondrites loses FeO, while chondrules become more FeO-rich rimwards with petrologic type (Huss et al. 1981 and

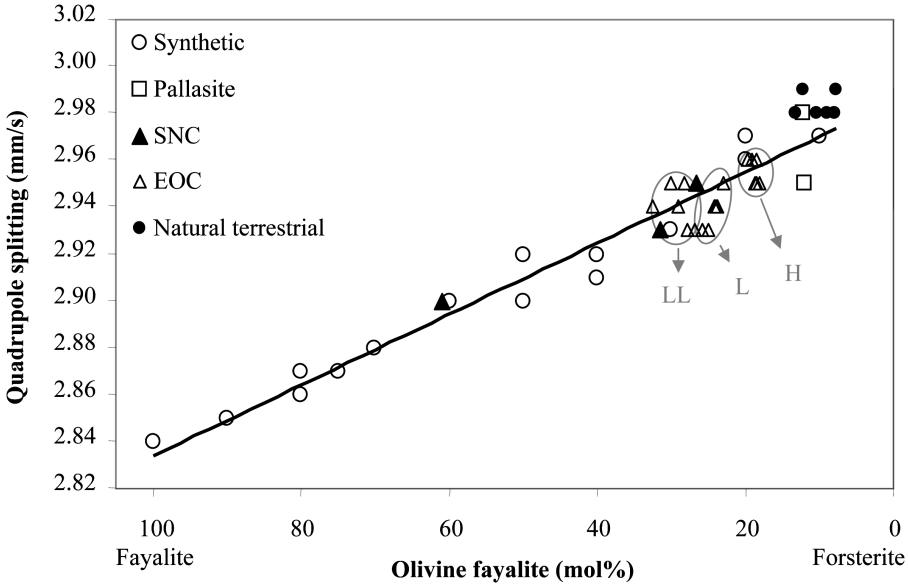

Fig. 7. Relationship between olivine composition (as fayalite mol%) and quadrupole splitting for synthetic and natural olivine samples (from Menzies et al. 2001). Errors on the quadrupole splitting data are <0.02 mm/s and are not included here in order to preserve the clarity of the figure. A linear best-fit line through the data is shown, the R^2 value is 0.94 (n = 50). SNC = Martian meteorites; EOC = equilibrated ordinary chondrites. The EOCs can be tentatively separated into a "H" and "L and LL" group on the basis of olivine quadrupole splitting.

McCoy et al. 1991). This is the result of diffusive chemical exchange with increasing temperature. Mössbauer analysis of bulk olivine (incorporating both chondrules and matrix) provides a more complete means of assessing total Fe movement. It suggests that along with a redistribution of Fe between matrix and chondrules, there is an overall trend of Fe loss from olivine during progressive metamorphism. The inference is that olivine undergoes reduction with metamorphism.

Olivine is the only mineral that can be readily analyzed in this manner as pyroxene does not show simple solid solution behaviour between two end-members and phyllosilicates have highly complex compositions and are not present in all samples. However, it is necessary to consider the entire mineral inventory of chondrites when discussing redox processes. There are a number of other ways in which the Mössbauer data can be used to investigate whether reduction is indeed affecting the entire sample.

Using the following oxidation reaction:

$$\underset{\text{metal}}{Fe} + \tfrac{1}{2}O_2 + \underset{\text{pyroxene}}{(Mg, Fe)SiO_3} \rightarrow \underset{\text{olivine}}{(Mg, Fe)_2SiO_4}$$

and the olivine and pyroxene abundances from Mössbauer spectroscopy (Table 1), we can predict whether oxidation or reduction is the more likely reaction affecting the silicates in UOCs. Again, we compare Mössbauer "percentages of fit" values for olivine and pyroxene. As they are concerned with the amount of total Fe contained in each mineral phase, the Mössbauer data provide a reliable means of investigating redox processes. Gastineau-Lyons et al. (2002) were not able to incorporate the UOCs into their oxidation model using this silicate ratio technique because quantitative modal mineralogy for UOCs has hitherto been inaccessible. By using silicate abundances from Mössbauer spectroscopy we hope to extend their observations. Figure 9 shows that when the olivine/pyroxene abundances for both falls and Antarctic finds are plotted against petrologic type, there is a clear decrease in the silicate ratio from type 3 to type 4. (Semarkona is the only exception to this trend with an olivine/pyroxene ratio of 1.1. This may be related to the comparatively higher proportion of phyllosilicate in this meteorite, which has modified the relative silicate proportions.) The data for type 5 and 6 EOCs do not show a continuation of this trend: thus the interpretation of this figure is synonymous with that provided for Fig. 8.

A literature investigation of other meteoritic components that might be sensitive to redox conditions tends to support the hypothesis that reduction occurred with metamorphism. Figure 10a shows the variation in carbon with petrologic type (Grady et al. 1982). As carbon is a potential reducing agent, its decrease with equilibration is entirely consistent with reduction occurring during metamorphism in the UOCs at least. Reduction owing to the presence of carbon on a parent body is known to lower the oxygen isotopic composition ($\delta^{18}O$) of EOCs owing to the depletion of heavy isotopes as CO and CO_2 gases are formed during heating (Clayton et al. 1991). Figure 10b shows the decrease in $\delta^{18}O$ in LL chondrites with progressive metamorphism. Figure 10c shows increasing Fe°/Fe_{total} with petrologic type (Jarosewich 1990), another indication of progressive reduction of UOCs and consistent with Fe loss from olivine. It is worth noting that Bishunpur, LL3.1, plots away from this trend. Average metal content for an LL fall is 2.44 wt% (Jarosewich 1990),

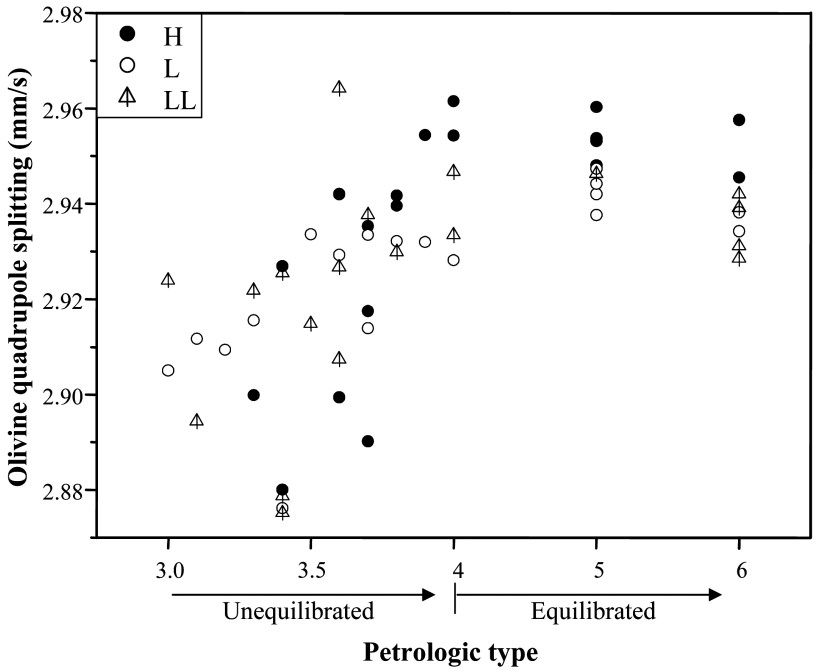

Fig. 8. A graph showing how quadrupole splitting values vary with increasing equilibration. Included are UOCs (both falls and Antarctic finds) and EOC falls. The scale on the x-axis is non-linear for reasons outlined in the text. Errors on the quadrupole splitting data are <0.02 mm/s.

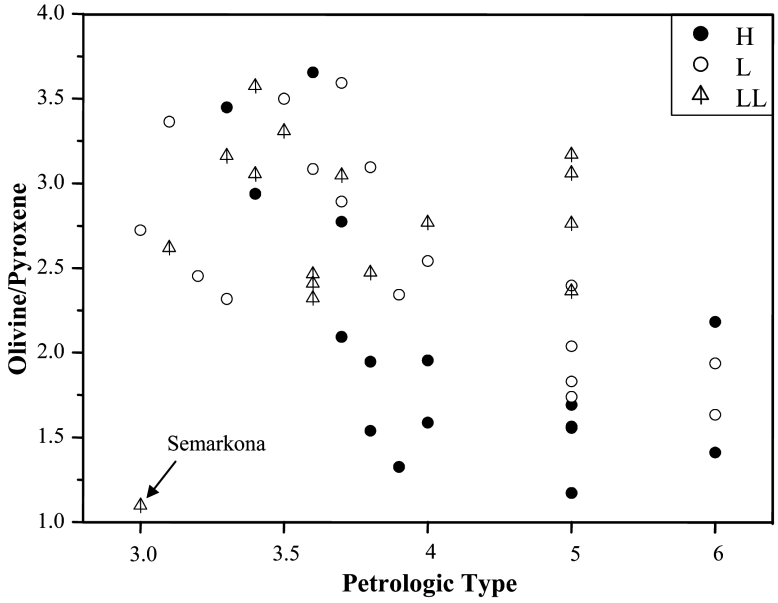

Fig. 9. A graph showing the variation in olivine/pyroxene ratio (from Mössbauer spectroscopy data). Both falls and Antarctic finds are shown. There is a broad decrease in olivine/pyroxene ratio with equilibration, suggesting reduction in the more unequilibrated ordinary chondrites. The EOCs do not follow this trend and may indicate that oxidation dominates in chondrites that have experienced more pronounced metamorphism.

while Bishunpur contains 14.1 wt% metal (by magnetic separation and weighing). This meteorite should be investigated in detail to confirm its assignment to the LL group. Finally, both the XRD and Mössbauer data indicate that magnetite only occurs in the most unequilibrated LL chondrites, suggesting that EOCs are the more reduced ordinary chondrites.

All of these separate lines of evidence indicate that there is a substantial change in redox reactions between the UOCs and EOCs, with a trend of increasing reduction in the UOCs followed by progressive oxidation in the EOCs. Figure 11 shows the proposed integrated model superimposed on a graph of olivine quadrupole splitting against petrologic type. The most primitive meteorites are the most oxidized,

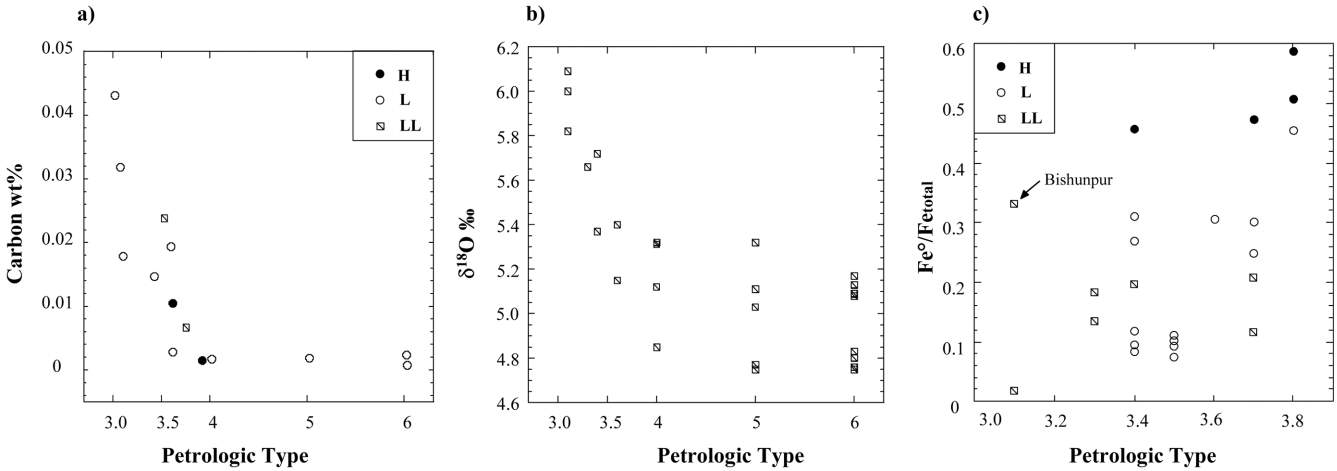

Fig. 10. Decreasing carbon wt% (a). Carbon released from stepped-combustion >500 °C (Grady et al. 1982); b) decreasing $\delta^{18}O$‰ (Clayton et al. 1991) with petrologic type, including both UOC and EOC LL falls. c) Increasing $Fe°/Fe_{total}$ with petrologic type in the UOCs, both falls and finds (Jarosewich 1990). Bishunpur has an elevated Fe° content for an LL chondrite and plots away from this trend (see text). These data are consistent with reduction occurring with increasing equilibration in the UOCs.

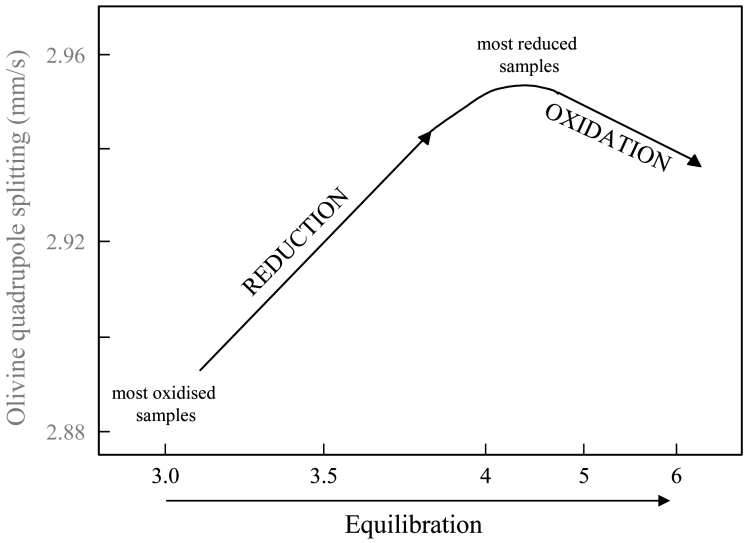

Fig. 11. Idealized scheme of increasing reduction through the UOCs followed by progressive oxidation in the EOCs. The model combines the observations of McSween and Labotka (1993) and Gastineau-Lyons et al. (2002) with our observations from Mössbauer spectroscopy. The graph is based on the olivine quadrupole splitting variation with petrologic type. (It must be noted that the scale on the x-axis is non-linear.) The most primitive meteorites retain original oxidation states imparted by the solar nebula. Reduction proceeds through the UOCs owing to the presence of a reducing agent, probably C. At temperatures sufficient to equilibrate type 3.9 and 4 chondrites, reduction ceases. There is a switch to progressive oxidation through the EOCs. However, it is evident that oxidation of the EOCs does not produce samples as oxidized as the most primitive type 3 material.

retaining oxidation states either imparted by the solar nebula or during very early aqueous alteration on the parent body. At temperatures sufficient to equilibrate type 3.9 and type 4 chondrites, reduction ceases. This temperature is estimated to be between 600° and 750 °C (Keil 2000). Progressive oxidation then occurs through the EOCs. While oxidation is the prevalent reaction in the EOCs, the EOCs themselves are the more reduced ordinary chondrites: they were never oxidized sufficiently to make them more oxidized than the original type 3 material.

When our observation are combined with the evidence of McSween and Labotka (1993) and Gastineau-Lyons et al. (2002) we can reconcile both end-members of equilibration and explain some of the apparently conflicting evidence described by previous workers. There is a trend of increasing reduction in the UOCs followed by progressive oxidation in the EOCs.

Our integrated model is in agreement with the observations of Larimer (1968) that reduction occurs with metamorphism in the UOCs. Heyse (1978) studied only

equilibrated LLs, so his observation that lower petrologic types (LL4) were more reduced than higher types (LL7) is consistent with the observation of McSween and Labotka (1993) that oxidation proceeds with metamorphism in the EOCs. Brett and Sato (1984) observed that the EOCs were more reduced than the UOCs. They compared a highly oxidized LL3.0 with an LL5 so the EOC would clearly be the more reduced sample. We cannot explain why the H6 sample they analyzed was more reduced than the H4. Had they extended their study to a larger sample set, it might have been possible to make more direct comparisons with our work.

It is necessary to explain why an environment of reduction would change to one of oxidation. If we assume that carbon is the primary reducing agent, then reduction of FeO in silicates to form Fe metal also produces CO and CO_2 gases that are lost by diffusion. Figure 10a shows that when temperatures equivalent to petrologic type 4 are reached, there is virtually no measurable carbon remaining in ordinary chondrites of any chemical class. Therefore it is reasonable to assume that reduction simply ceases when the supply of carbon is depleted. Additionally Brett and Sato (1984) noted that carbon becomes dissolved in Fe-Ni metal at high temperatures thus diminishing its reducing potential in EOCs. With increasing temperature and pressure, the solubility of carbon in metal increases so that at temperatures of 730 °C Fe metal can contain up to 1% carbon (Wood 1993).

It is also interesting that the temperature of culmination of reduction is coincident with the end of dehydration of hydrous phases. Fe-containing phyllosilicates in UOCs are dehydrated to ferromagnesian silicates with increasing temperature, as described in Fig. 5, effectively converting Fe^{3+} (in phyllosilicates) to Fe^{2+} (in olivine and pyroxene) and then Fe^{2+} is reduced to Fe^0 in metal. When dehydration is completed at temperatures of approximately 700 °C (Malysheva 1994), the supply of Fe^{2+} from phyllosilicates ceases, thus terminating the reduction processes.

At temperatures greater than petrologic type 4, no available carbon exists (and all phyllosilicates have been dehydrated), thus Fe metal will be available for oxidation, increasing the Fe contents of silicates as described by McSween and Labotka (1993) and Gastineau-Lyons et al. (2002). This eliminates the necessity to invoke selective oxidation in the EOCs by externally derived oxidizing vapors (McSween and Labotka 1993).

CONCLUSIONS

This work provides the first quantification of the modal mineralogy of unequilibrated ordinary chondrites, using a combination of Mössbauer spectroscopy and X-ray diffraction. Apart from being a novel experimental technique, our study yields information about the circumstances of ordinary chondrite metamorphism. Mössbauer spectroscopy is a useful preliminary tool for identifying minerals such as clay and magnetite, while with XRD we can fine-tune the quantification. The changing mineralogy provides information about how aqueous alteration and dehydration proceed with metamorphism on meteorite parent bodies. Furthermore, Mössbauer spectroscopy allows us to make other observations about early conditions, such as redox state, on chondrite parent bodies.

Some important conclusions from this integrated approach are:

1. UOCs contain primary phyllosilicate material, which we propose underwent dehydration to form ferromagnesian silicates during progressive metamorphism.
2. The combined use of Mössbauer spectroscopy and XRD in this study identifies a larger proportion of phyllosilicate material in UOCs than other petrographic studies. We propose that this is the consequence of incipient alteration along silicate structures and defects on the nm scale that can be observed using TEM.
3. UOCs underwent significant reduction during metamorphism, a process that can be identified using the Mössbauer parameters of silicates and the ratios of olivine and pyroxene as observed by Mössbauer spectroscopy. Both these techniques allow, for the first time, a detailed comparison to be made between the redox states in UOCs and EOCs.
4. Bishunpur appears to be an unusual LL chondrite containing a significantly higher proportion of Fe-Ni metal than other LL chondrites. It also contains a large proportion of both pure forsterite and pure fayalite and no primary magnetite (a common phase in other oxidized UOC falls). Perhaps the classification of this meteorite should be reviewed.

As the meteorite community are now in possession of such a large database of chemical analyses and mineralogical observations, we should work towards quantifying the mineralogy of all primitive chondrites. This information can then be integrated in order to model geological processes on meteorite parent bodies. Given that little was known about the mineral compliment of UOCs prior to this work, it is possible that asteroidal spectral data should be re-interpreted with these new data in mind.

Acknowledgments–P. A. Bland would like to thank the Royal Society and PPARC for their support. This paper is IARC Publication #2005-0726.

Editorial Handling—Dr. Hiroko Nagahara

REFERENCES

Alexander C. M. O'D., Barber D. J., and Hutchison R. 1989. The microstructure of Semarkona and Bishunpur. *Geochimica et Cosmochimica Acta* 53:3045–3057.

Banfield J. F., Veblen D. R., and Jones B. F. 1990. Transmission electron microscopy of subsolidus oxidation and weathering of

olivine. *Contributions to Mineralogy and Petrology* 106:110–123.
Batchelder M. and Cressey G. 1998. Rapid, accurate phase quantification of clay-bearing samples using a position-sensitive X-ray detector. *Clays and Clay Minerals* 46:183–194.
Berry F. J. 1983. Mössbauer spectroscopy: 25 years after the discovery. *Physics Bulletin* 34:517–519.
Bish D. L. and Howard S. A. 1988. Quantitative phase analysis using the Rietveld method. *Journal of Applied Crystallography* 21:86–91.
Bland P. A. and Cressey G. 2001. Modal mineralogy of unequilibrated chondrites by X-ray diffraction and Mössbauer spectroscopy (abstract #1853). 32nd Lunar and Planetary Science Conference. CD-ROM.
Bland P. A., Smith T. B., Jull A. J. T., Berry F. J., Bevan A. W. R., Cloudt S., and Pillinger C. T. 1996. The flux of meteorites to the Earth over the last 50,000 years. *Monthly Notices of the Royal Astronomical Society* 283:551–565.
Bland P. A., Sephton M. A., Bevan A. W. R., Berry F. J., Cadogan J. M., and Pillinger C. T. 1997. Magnetite in Vigarano: An ^{57}Fe Mössbauer spectroscopic study. LPI Technical Report #97-02. Houston, Texas: Lunar and Planetary Science Institute. pp. 3–5.
Bland P. A., Sexton A. S., Jull A. J. T., Bevan A. W. R., Berry F. J., Thornley D. M., Astin T. R., Britt D. T., and Pillinger C. T. 1998. Climate and rock weathering: A study of terrestrial age dated ordinary chondritic meteorites from hot desert regions. *Geochimica et Cosmochimica Acta* 62:3169–3184.
Bland P. A., Lee M. R., Sexton A. S., Franchi I. A., Fallick A. E. T., Miller M. F., Cadogan J. M., Berry F. J., and Pillinger C. T. 2000. Aqueous alteration without a pronounced oxygen-isotopic shift: Implications for the asteroidal processing of chondritic materials. *Meteoritics & Planetary Science* 35:1387–1395.
Bland P. A., Cressey G., and Menzies O. N. 2002. A continuum of aqueous alteration in the carbonaceous chondrites (abstract). *Meteoritics & Planetary Science* 37:A18.
Bland P. A., Cressey G., and Menzies O. N. 2004. Modal mineralogy of carbonaceous chondrites by X-ray diffraction and Mössbauer spectroscopy. *Meteoritics & Planetary Science* 39:3–16.
Brearley A. J. and Jones R. H. 1998. Chondritic meteorites. In *Planetary materials, reviews in mineralogy,* edited by J. J. Papike. Washington, D.C.: Mineralogical Society of America. pp. 3-83–3-370.
Brett R. and Sato M. 1984. Intrinsic oxygen fugacity measurements on seven chondrites, a pallasite, and a tektite and the redox state of meteorite parent bodies. *Geochimica et Cosmochimica Acta* 48:111–120.
Burns R. G. 1993. Mössbauer spectral characterisation of iron in planetary surface materials. In *Topics in remote sensing 4. Remote geochemical analysis: Elemental and mineralogical composition,* edited by. Pieters C. M and Englert P. A. J. Cambridge: Cambridge University Press.
Chung F. H. 1974a. Quantitative interpretation of X-ray diffraction patterns of mixtures. I. Matrix-flushing method for quantitative multicomponent analysis. *Journal of Applied Crystallography* 7: 519–525.
Chung F. H. 1974b. Quantitative interpretation of X-ray diffraction patterns of mixtures. II. Adiabatic principle of X-ray diffraction analysis of mixtures. *Journal of Applied Crystallography* 7:526–531.
Clayton R. N., Mayeda T. K., Goswami J. N., and Olsen E. J. 1991. Oxygen isotope studies of ordinary chondrites. *Geochimica et Cosmochimica Acta* 55:2317–2337.
Cressey G. and Batchelder M. 1998. Dealing with absorption and microabsorption in quantitative phase analysis. In, Comission for Powder Diffraction. *International Union of Crystallography Newsletter* 20:16–17.
Cressey G. and Schofield P. F. 1996. Rapid whole-pattern profile-stripping method for the quantification of multiphase samples. *Powder Diffraction* 11:35–39.
Dodd R. T. 1969. Metamorphism of the ordinary chondrites: A review. *Geochimica et Cosmochimica Acta* 33:161–203.
Dodd R. T. 1981. *Meteorites. A petrologic-chemical synthesis,* Cambridge, England: Cambridge University Press. 368 p.
Dodd R. T., van Schmus W. R., and Koffman D. M. 1967. A survey of the unequilibrated ordinary chondrites. *Geochimica et Cosmochimica Acta* 31:921–951.
Dorfler G. and Hiesbock H. G. 1969. Investigations on a quantitative mineralogical characterization of meteorites by modal analysis. In *Meteorite research,* edited by Millman P. A. Dordrecht, The Netherlands: Reidel Publishing Company.
DuFresne E. R. and Anders E. 1961. On the chemical evolution of the carbonaceous chondrites. *Geochimica et Cosmochimica Acta* 26: 1085–1114.
Easton A. J. and Elliot C. J. 1977. Analyses of some meteorites from the British Museum Natural History collection. *Meteoritics* 12: 409–416.
Eggleton R. A. 1984. Formation of iddingsite rims on olivine: A transmission electron microscope study. *Clays and Clay Minerals* 32:1–11.
Fegley Jr. B., Lodders K., Treiman A. H., and Klingelhofer G. 1995. The rate of pyrite decomposition on the surface of Venus. *Icarus* 115:159–180.
Gastineau-Lyons H. K., McSween H. Y., Jr., and Gaffey M. J. 2002. A critical evaluation of oxidation versus reduction during metamorphism of L and LL group chondrites, and implications for asteroid spectroscopy. *Meteoritics & Planetary Science* 37: 75–89.
Gooding J. L. 1986. Clay-mineraloid weathering products in Antarctic meteorites. *Geochimica et Cosmochimica Acta* 50: 2215–2223.
Grady M. M. 2000. *Catalogue of meteorites,* 2nd edition. Cambridge: Cambridge University Press. 689 p.
Grady M. M., Swart P. K., and Pillinger C. T. 1982. Carbon isotopic composition of some type 3 ordinary chondrites (abstract). 13th Lunar and Planetary Science Conference. pp. 277–278.
Grossman J. N., Alexander C. M. O'D., Wang J., and Brearly A. J. 2000. Bleached chondrules: Evidence for widespread aqueous processes on the parent asteroids of ordinary chondrites. *Meteoritics & Planetary Science* 35:467–486.
Herr W. and Skerra B. 1969. Mössbauer spectroscopy applied to the classification of stone meteorites. In *Meteorite research,* edited by Millman P. A. Dordrecht, The Netherlands: Reidel Publishing Company.
Heyse J. V. 1978. The metamorphic history of LL-group ordinary chondrites. *Earth and Planetary Science Letters* 40:365–381.
Hill R. J. and Howard C. J. 1987. Quantitative phase analysis from neutron powder diffraction using Rietveld method. *Journal of Applied Crystallography* 20:467–474.
Hochella M. F. J. and Banfield J. F. 1995. Chemical weathering of silicates in nature: A microscopic perspective with theoretical considerations. In *Chemical weathering rates of silicate minerals,* edited by White A. F. and Brantley S. L. Washington, D.C: Mineralogical Society of America.
Huss G. R., Keil K., and Taylor G. J. 1981. The matrices of unequilibrated ordinary chondrites: Implications for the origin and history of chondrites. *Geochimica et Cosmochimica Acta* 45: 33–51.
Hutchison R., Bevan A. W. R., Easton A. J., and Agrell S. O. 1981. Mineral chemistry and genetic relations among H-chondrites. *Proceedings of the Royal Society of London A* 374:159–178.
Hutchison R. T., Alexander C. M. O'D., and Barber D. J. 1987. The

Semarkona meteorite: First recorded occurrence of smectite in an ordinary chondrite, and its implications. *Geochimica et Cosmochimica Acta* 51:1875–1882.

Jarosewich E. 1966. Chemical analyses of ten stony meteorites. *Geochimica et Cosmochimica Acta* 30:1261–1265.

Jarosewich E. 1990. Chemical analyses of meteorites: A compilation of stony and iron meteorite analyses. *Meteoritics* 25:323–337.

Keil K. 2000. Thermal alteration of asteroids: Evidence from meteorites. *Planetary and Space Science* 48:887–903.

Krot A. N., Scott E. R. D., and Zolensky M. E. 1997. Origin of fayalitic olivine rims and lath-shaped matrix olivine in the CV3 chondrite Allende and its dark inclusions. *Meteoritics & Planetary Science* 32:31–49.

Larimer J. W. 1968. Experimental studies on the system Fe-MgO-SiO_2-O_2 and their bearing on the petrology of the chondritic meteorites. *Geochimica et Cosmochimica Acta* 32:1187–1207.

Malysheva T. V. 1994. Mössbauer study of redox processes in the evolution of chondrites. *Mineralogical Magazine* 58:151–158.

McCoy T. J., Scott E. R. D., Jones R. H., Keil K., and Taylor G. J. 1991. Composition of chondrule silicates in LL3-5 chondrites and implications for their nebular history and parent body metamorphism. *Geochimica et Cosmochimica Acta* 55:601–619.

McSween H. Y., Bennett M. E., and Jarosewich E. 1991. The mineralogy of ordinary chondrites and implications for asteroid spectrophotometry. *Icarus* 90:107–116.

McSween H. Y. and Labotka T. C. 1993. Oxidation during metamorphism of the ordinary chondrites. *Geochimica et Cosmochimica Acta* 57:1105–1114.

Meisel W., Griesbach P., Grabke H. J., and Gutlich P. 1990. Quantitative determination of fayalite layers on iron by CEMS. *Hyperfine Interactions* 57:2001–2008.

Menzies O. N., Bland P. A., and Berry F. J. 2001. An ^{57}Fe Mössbauer study of the olivine solid solution series: Implications for meteorite classification and deconvolution of unequilibrated chondrite spectra (abstract #1622). 32nd Lunar and Planetary Science Conference. CD-ROM.

Rubin A. E. 1990. Kamacite and olivine in ordinary chondrites: Intergroup and intragroup relationships. *Geochimica et Cosmochimica Acta* 54:1217–1232.

Schofield P. F., Knight K. S., Covey-Crump S. J., Cressey G., and Stretton I. C. 2002. Accurate quantification of the modal mineralogy of rocks when image analysis is difficult. *Mineralogical Magazine* 66:189–200.

Sears D. W., Grossman J. N., and Melcher C. L. 1982. Chemical and physical studies of type 3 chondrites—I: Metamorphism related studies of Antarctic and other type 3 ordinary chondrites. *Geochimica et Cosmochimica Acta* 46:2471–2481.

Sears D. W., Grossman J. N., Melcher C. L., Ross L. M., and Mills A. A. 1980. Measuring metamorphic history of unequilibrated ordinary chondrites. *Nature* 287:791–795.

Sears D. W. G. and Akridge D. G. 1998. Nebular or parent body alteration of chondritic material: Neither or both? *Meteoritics & Planetary Science* 33:1157–1167.

Sears D. W. G. and Weeks K. S. 1986. Chemical and physical studies of type 3 chondrites-VI: Siderophile elements in ordinary chondrites. *Geochimica et Cosmochimica Acta* 50:2815–2832.

Sears D. W. G. and Hasan F. A. 1987. The type three ordinary chondrites: A review. *Surveys in Geophysics* 9:43–97.

Smith K. L., Milnes A. R., and Eggleton R. A. 1987. Weathering of basalt: Formation of iddingsite. *Clays and Clay Minerals* 35: 418–428.

Sprenkel-Segel E. L. and Hanna S. S. 1964. Mössbauer analysis of iron in stone meteorites. *Geochimica et Cosmochimica Acta* 28: 1913–1931.

van Schmus W. R. and Wood J. A. 1967. A chemical-petrologic classification for the chondritic meteorites. *Geochimica et Cosmochimica Acta* 31:747–765.

Wood B. J. 1993. Carbon in the core. *Earth and Planetary Science Letters* 117:593–607.

Zolensky M. and McSween H. Y., Jr. 1988. Aqueous alteration. In *Meteorites and the early solar system,* edited by Kerrridge J. F. and Matthews M. S. Tucson, Arizona: The University of Arizona Press. 1269 p.